Morpho-molecular traits of Indo-Pacific and Caribbean Halofolliculina ciliate infections

Montano, Simone; Maggioni, Davide; Liguori, Giulia; Arrigoni, Roberto; Berumen, Michael L.; Seveso, Davide; Galli, Paolo; Hoeksema, Bert W.

Published in:
Coral Reefs

DOI:
10.1007/s00338-020-01899-6

Publication date:
2020

Coral Reefs (2020) 39:375–386
https://doi.org/10.1007/s00338-020-01899-6

REPORT

Morpho-molecular traits of Indo-Pacific and Caribbean *Halofolliculina* ciliate infections

Simone Montano[1,2] · Davide Maggioni[1,2] · Giulia Liguori[1,2] · Roberto Arrigoni[3,4,5] · Michael L. Berumen[5] · Davide Seveso[1,2] · Paolo Galli[1,2] · Bert W. Hoeksema[6,7]

Received: 1 July 2019 / Accepted: 27 January 2020 / Published online: 5 February 2020

Abstract Coral diseases are emerging as a major threat to coral reefs worldwide, and although many of them have been described, knowledge on their epizootiology is still limited. This is the case of the *Halofolliculina* ciliate infections, recognized as the skeletal eroding band (SEB) and Caribbean ciliate infection (CCI), two diseases caused by ciliates belonging to the genus *Halofolliculina* (Class Heterotrichea). Despite their similar macroscopic appearance, the two diseases are considered different and their pathogens have been hypothesized to belong to different *Halofolliculina* species. In this work, we analysed the morphology and genetic diversity of *Halofolliculina* ciliates collected in the Caribbean Sea, Red Sea and Indo-Pacific Ocean. Our analyses showed a strong macroscopic similarity of the lesions and similar settlement patterns of the halofolliculinids from the collection localities. In particular, the unique erosion patterns typical of the SEB were observed also in the Caribbean corals. Fine-scale morphological and morphometric examinations revealed a common phenotype in all analysed ciliates, unequivocally identified as *Halofolliculina corallasia*. Phylogenetic analyses based on nuclear and mitochondrial (COI) molecular markers consistently found all samples as monophyletic. However, although the nuclear marker displayed an extremely low intra-specific diversity, consistent with the morphological recognition of a single species, the analyses based on COI showed a certain level of divergence between samples from different localities. Genetic distances between localities fall within the intra-specific range found in other heterotrich ciliates, but they may also suggest the presence of a *H. corallasia* species complex. In conclusion, the presented morpho-molecular characterization of *Halofolliculina* reveals strong similarities between the pathogens causing SEB and CCI and call for further detailed studies about the distinction of these two coral diseases.

Topic Editor Carly Kenkel

Electronic supplementary material The online version of this article (https://doi.org/10.1007/s00338-020-01899-6) contains supplementary material, which is available to authorized users.

✉ Simone Montano
simone.montano@unimib.it

[1] Department of Earth and Environmental Sciences (DISAT), University of Milan – Bicocca, Piazza della Scienza, 20126 Milan, Italy

[2] MaRHE Center (Marine Research and High Education Center), Magoodhoo Island, Faafu Atoll, Republic of Maldives

[3] Department of Biology and Evolution of Marine Organisms (BEOM), Stazione Zoologica Anton Dohrn Napoli, Villa Comunale, 80121 Naples, Italy

[4] European Commission, Joint Research Centre (JRC), Ispra, Italy

[5] Division of Biological and Environmental Science and Engineering, Red Sea Research Center, King Abdullah University of Science and Technology, Thuwal 23955-6900, Saudi Arabia

[6] Taxonomy and Systematics Group, Naturalis Biodiversity Center, P.O. Box 9517, 2300 RA Leiden, The Netherlands

[7] Groningen Institute for Evolutionary Life Sciences, University of Groningen, P.O. Box 11103, 9700 CC Groningen, The Netherlands

Keywords Ciliate · Protozoan · Syndrome · *Halofolliculina corallasia* · Coral reefs · Scleractinian corals

Introduction

Coral reefs are declining worldwide, with an estimated coral cover loss of 50% in the Indo-Pacific and 80% in the Caribbean over the last 30 years (Gardener et al. 2003; Bruno and Selig 2007; Pollock et al. 2011). The causes of this decline are multiple and complex, with coral diseases emerging as one of the most affecting threats (Rosenberg et al. 2007; Bourne et al. 2009; Sutherland et al. 2015).

Currently, it is not clear how many coral diseases exist globally, and a certain level of confusion emerges from the incomplete information reported in the literature (Willis et al. 2004). Indeed, despite their negative impact, the majority of coral diseases remain a mystery, as a result of the limited analytic methods, the poor knowledge of the putative pathogens and the consequent deficiency of epizootiological data (Work and Meteyer 2014; Bourne et al. 2015). One of the most dramatic and recent examples is the Stony Coral Tissue Loss Disease (SCTLD), which has been affecting various coral species along the Florida Reef Tract since 2014 (Aeby et al. 2019). Although its effect is unprecedented, all the efforts carried out by research have so far not been successful in discovering its causative agents (Meyer et al. 2019). The lack of specific and accurate diagnostic tools coupled with difficulties encountered in the study of bacteria-based diseases resulted also in ambiguous classifications of coral diseases that remain largely open to interpretation (Pollock et al. 2011). The shortage of multidisciplinary approaches to describe coral lesions and to identify morphologically and molecularly the pathogens have led to recognize a high number of possibly different diseases, which often share similar gross morphology of the lesions, as for the Indo-Pacific White Syndromes (Bourne et al. 2015). Furthermore, in some cases, diseases were named differently, even if caused by the same putative pathogens. This is the case of the Black Band Disease (BBD) and the Red Band Disease (RBD) of Palau, in which the filamentous cyanobacteria forming red and black bands were molecularly identified as belonging to a single ribotype only after their isolation, culturing and sequencing (Sussman et al. 2006). Moreover, this scenario is further complicated by the existence of coral diseases caused by a consortium of pathogens that may slightly differ among geographic areas. Therefore, the BBD, recognized as a worldwide distributed disease caused by a consortium of microorganism dominated by a cyanobacterial component, may differ in its predominant portion between the Caribbean and Indo-Pacific (Casamatta et al. 2012).

The skeletal eroding band (SEB) is one of the first coral diseases detected and described from the Indo-Pacific coral reefs (Antonius 1999). It is caused by the folliculinid ciliate *Halofolliculina corallasia* Antonius and Lipscomb (2001) (Class Heterotrichea; Order Heterotrichida), which not only attacks the soft tissues of corals but also damages their skeleton (Antonius and Lipscomb 2001; Riegl and Antonius 2003; Page and Willis 2008). In *H. corallasia*, the lorica (sac-like housing) has a rounded posterior and a cylindrical neck that angles up from the surface at about 45°, and it has an average length and width of 220 µm and 95 µm, respectively. They are settled on the coral skeleton, usually following the rim of the corallites, and in most cases, only the neck rises above the coral surface. The disease manifests as a dark-grey band 1–10 cm thick, located at the interface between recently exposed skeleton and apparently healthy coral tissue. The SEB has been recorded affecting 82 scleractinian species on various Indo-Pacific and Red Sea coral reefs, with the most affected taxa being branching species of *Acropora* and *Pocillopora* (Page et al. 2015). According to these data, the SEB shows the widest host range of any coral disease recorded to date, reaching the top on the list of harmful coral syndromes (reviewed by Page and Willis 2008).

In 2004–2005, a similar ciliate infection was reported from 25 out of about 60 Caribbean coral species (Cróquer et al. 2006a; Page et al. 2015), in which the infection appeared as a dark band located between healthy tissue and bare skeleton, showing, on closer inspection, the characteristic spotted appearance of the clustering ciliates (Cróquer et al. 2006a). The general morphology of the Caribbean ciliate is very similar to that of *Halofolliculina corallasia* from the Indo-Pacific (Cróquer et al. 2006b; Rodríguez et al. 2009). Both ciliates have a free-living phase that moves towards living tissues, penetrates them and attaches itself, and a sessile form settled in a lorica, with the cell body attached at its pointed posterior end, showing two conspicuous pericytostomial wings bearing feeding cilia (Antonius 1999; Antonius and Lipscomb 2001; Cróquer et al. 2006b).

Despite a similar fine-scale morphology among *Halofolliculina* ciliates affecting Indo-Pacific and Caribbean corals, the skeletal erosion is often associated with SEB, but not with the Caribbean ciliate infections to date (Page et al. 2015). However, no information is present in the literature about the apparent no-eroding pattern of ciliate affecting Caribbean corals, leaving space for additional in-depth studies.

Initially, it was proposed that these ciliates might have recently invaded the Caribbean from the Indo-Pacific region (Cróquer et al. 2006b), but then the authors stated

that the Caribbean and Indo-Pacific ciliates are different species, based on unpublished data (Cróquer et al. 2006a). Despite the Caribbean pathogen is still to be formally characterized and described at species level, researchers suggested the name Caribbean ciliate infections (CCI) to indicate the presumed new disease, due to the apparent differences in aetiology (Weil and Hooten 2008; Rodríguez et al. 2009; Weil and Rogers 2011). By contrast, it has also been reported by Sweet and Séré (2015) that SEB and CCI are caused by the same pathogen, despite an absence of evidence to support this conclusion.

Therefore, the goal of this study is to improve the knowledge concerning the *Halofolliculina* ciliate infections (sensu Page et al. 2015) by investigating the aetiology of SEB and CCI through a morpho-molecular approach, in order to assess and confirm possible taxonomic affinities between the *Halofolliculina* species.

Materials and methods

Sampling was conducted between June 2017 and October 2019 in three geographic areas, including the Indian Ocean (Republic of the Maldives), the Red Sea (Saudi Arabia) and the Caribbean Sea (Curaçao and Bonaire) (Fig. 1).

The presence of the *Halofolliculina* ciliate infection was qualitatively recorded both by snorkelling and SCUBA diving through a roving technique (Hoeksema and Koh 2009). A dive of approximatively one hour was carried out at each sampling locality, starting from a maximum depth of 10–25 m and moving towards shallower waters. In each locality, two to four small diseased coral fragments were taken with a hammer and chisel from colonies showing the characteristic band. Underwater photographs were taken using a Canon GX7 Mark II camera in a Fantasea GX7 II underwater housing. Diseased coral colonies used in the study were chosen randomly (depending on their abundance) and include *Pocillopora* spp. and *Porites lutea* in the Indo-Pacific and the Red Sea, and *Eusmilia fastigiata* and *Diploria labyrinthiformis* in the Caribbean Sea. After a preliminary observation, samples were fixed in formalin 6% and ethanol 99%, for further morphological and molecular analyses, respectively.

Halofolliculinid protozoans were initially observed in vivo with a Leica EZ4 D stereomicroscope to examine the protozoan aggregations and to search for possible macroscopic differences, such as a different colouration and the shape of the lorica. Then, single individuals were detached from the coral skeleton using needles, precision forceps and micropipettes and placed on a glass slide to observe their morphology at higher magnification under a Zeiss Axioskop 40 microscope. Subsequently, ten coral fragments belonging to the four genera (*Diploria*, *Eusmilia*, *Pocillopora*, *Porites*) were observed using both the Tescan Vega TS 5136 XM scanning electron microscope, operating at beam energies of 20 kV, and the Zeiss Gemini SEM500 scanning electron microscope operating at beam energies of 5 kV. About 30 loricae were randomly chosen for each coral fragment to take measurements of the diameter, length and width of both the neck and the ampulla, according to Antonius and Lipscomb (2001) and Primc-Habdija and Matonickin (2005) (Fig. S1). Measurements were recorded using the Scanning Electron Microscope measuring software SmartSEM (ZEISS, Oberkochen, Germany) with maximum resolution of 1 nm. Additionally, a preliminary characterization of the skeletal erosion caused by the CCI has also been carried out through SEM imaging.

The morphometric measurements were tested for normality distribution with a Shapiro–Wilk test of normality. One-way analyses of variance (ANOVA) were performed to test for differences in the neck diameter between localities, whereas differences in the length of the neck and diameter of the neck brim were tested using a nonparametric Kruskal–Wallis test, since the data were not normally distributed (Zar 1999). Ampullae length and width of *Halofolliculina* loricae were analysed by descriptive statistics due the few observations obtained. Statistical analyses were performed using SPSS ver. 24 (IBM, New York). All data are presented as mean ± standard error (SE), unless otherwise stated.

Molecular analyses

The genomic DNA was extracted following a protocol already successfully used for different taxa (Montano et al. 2015; Beli et al. 2018). Two molecular markers were amplified, namely a portion of the nuclear ITS (~ 400 bp) and the mitochondrial COI gene (~ 600 bp), following the protocols described in Fernandes et al. (2016) and Strüder-Kypke and Lynn (2010), respectively. These two DNA regions where chosen because they are generally considered reliable markers to infer ciliate phylogeny (e.g. Sun et al. 2010; Yi and Song 2011; Fernandes et al. 2016) and because they show different substitution rates, with the COI being the more variable marker and having been already used to assess ciliates intra-specific variability (e.g. Gentekaki and Lynn 2009; Strüder-Kypke and Lynn 2010). The amplicons were purified and sequenced in both forward and reverse directions using a DNA Analyser 3730xl (Applied Biosystems, California, USA). The obtained sequences were imported, assembled, and visually checked into Geneious R7. For each molecular marker, a dataset was assembled adding sequences belonging to halofolliculinid relatives downloaded from GenBank. Sequences from two karyorelictid species (*Corlissina maricaensis,*

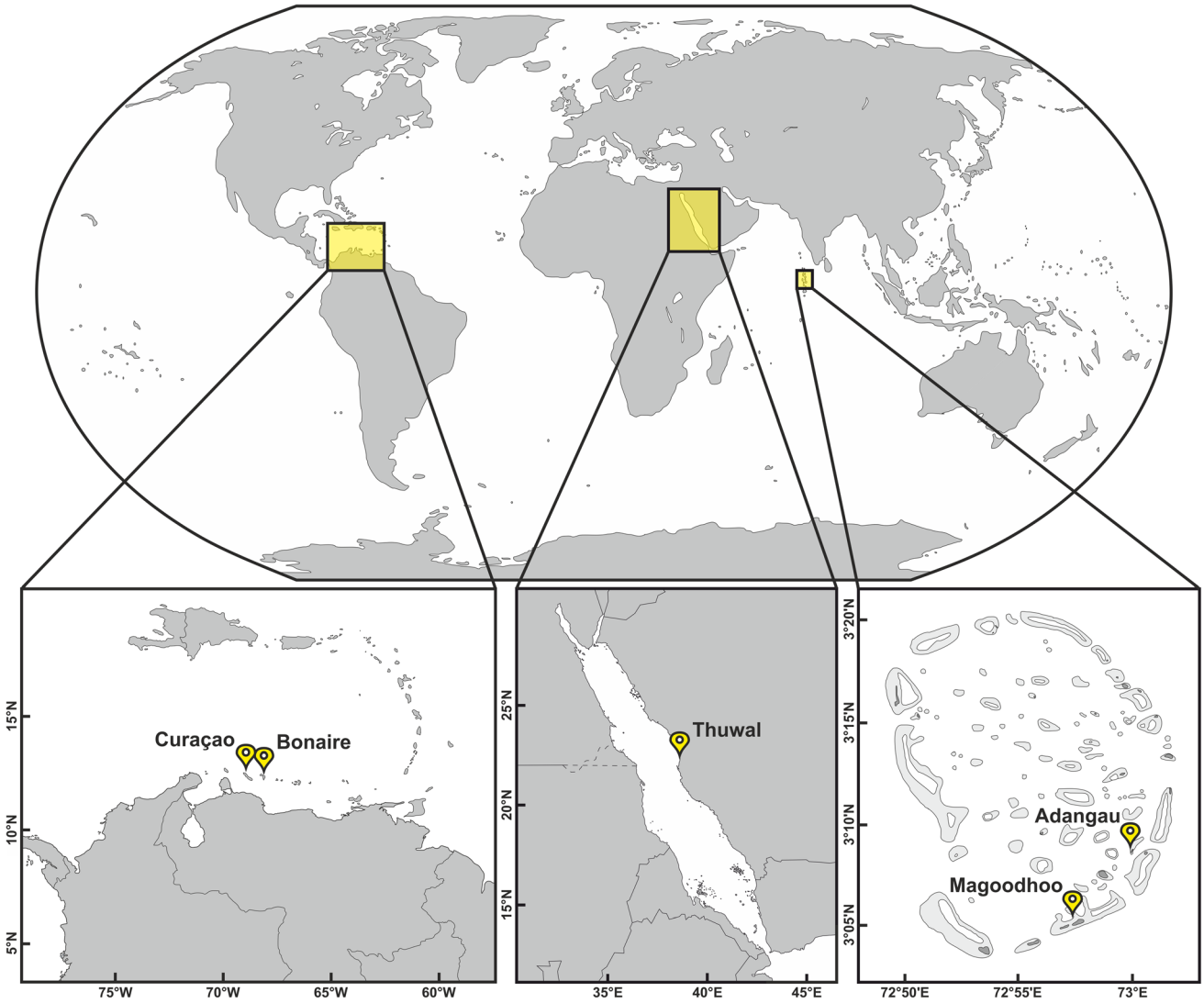

Fig. 1 Sampling localities in the Caribbean Sea (Curaçao and Bonaire), Red Sea (Saudi Arabia), and Indo-Pacific (Republic of the Maldives)

Loxodes vorax) were also included as outgroups. Sequences were aligned using the E-INS-i option in MAFFT 7.402 (Katoh and Standley 2013), and were then run through Gblocks (Castresana 2000; Talavera and Castresana 2007) to remove low quality and ambiguously aligned positions. Phylogenetic analyses were performed using Bayesian Inference (BI) and Maximum Likelihood (ML). JmodelTest2 2.1.6 (Darriba et al. 2012) was run to find the proper molecular models, and the best-fitting model selected for both datasets was GTR+G, as suggested by the Aikaike Information Criterion (AIC). BI analyses were performed using MrBayes 3.2.6 (Ronquist et al. 2012): four parallel Markov Chain Monte Carlo runs (MCMC) were run for 10^7 generations, trees were sampled every 1000th generation, and burn-in was set to 25%. ML analyses were performed with RAxML v8.2.10 (Stamatakis 2006, 2014) using 1000 bootstrap replicates. Resulting trees were displayed and edited using FigTree 1.4.0 (Rambaut 2012) and CorelDraw X7 (Corel Corporation, Ottawa, Canada). Genetic distances (uncorrected *p*-distances, 1000 bootstrap) among and within heterotrich lineages were obtained for both molecular markers using MEGA-X (Kumar et al. 2018). The obtained sequences were deposited in GenBank (accession numbers ITS: MN829871-MN829873; COI: MN905752-MN905758) with relative sample codes and sampling sites.

Results

Morphological results

Our ecological surveys reveal the presence of *Halofolliculina* ciliate infections diseases in all three investigated

areas. First examinations revealed clusters of protozoans placed on coral surface between recently exposed skeleton and apparently healthy coral tissues, forming dense bands characterized by a dark green, almost black, colour pattern in diseased corals from both the Caribbean and the Indo-Pacific (Fig. 2a, b). In all samples, protozoans matched the description of *Halofolliculina corallasia* provided by Antonius and Lipscomb (2001). The body was covered by rows of cilia and showed the two characteristic bifurcate pericystomial wings bearing the oral polykinetids (Fig. 2c, d).

To better visualize the morphology of the loricae and to confirm their identification, a total number of 109 loricae (24 on *Porites lutea*, 29 on *Eusmilia fastigiata*, 10 on *Diploria labyrinthiformis*, 35 on *Pocillopora damicornis,* and 11 on *Pocillopora verrucosa*) were examined using the SEM. All the loricae had a rounded posterior and a cylindrical neck with a single sculpture line circumscribing it (Fig. 3). Furthermore, no significative differences in the overall distribution, settlement patterns and general size of the loricae have been observed between the coral genera and localities investigated. In general, the mean ampulla length (l) and width (w) were higher in the Caribbean samples (l = 146.4 ± 4.3 µm; w = 83.3 ± 6.2 µm) compared to the Maldivian specimens (l = 112.7 ± 4.1 µm; w = 62.1 ± 4.7 µm) and the Red Sea specimens (l = 54.3 µm; w = 51.1 µm). Regarding the length of the neck, mean values of 40.1 ± 1.0 µm and 40.9 ± 3.1 µm were observed in the Maldivian and Red Sea specimens, respectively, whereas a mean value of 32.2 ± 1.1 µm was observed for the Caribbean ciliates. Furthermore, similar values were found for the neck diameter, with Maldivian, Red Sea and Caribbean ciliates showing mean values of 31.25 ± 0.9 µm, 32.28 ± 0.9 µm and 31.20 ± 1.0 µm, respectively (Fig. 4).

According to the parametric and nonparametric tests performed, the neck diameters and neck lengths were not statistically different between the three geographic areas (neck diameters: ANOVA $F_{2,90}$ = 0.406, p = 0.668; neck length: Kruskal–Wallis H = 6.06 p = 0.051). In contrast, a significant difference was observed for the neck brim diameter between the three geographic areas, with the Maldivian specimens showing a mean value of 42.2 ± 1.4 µm, the Red Sea of 45.5 ± 1.0 µm and the Caribbean of 46.9 ± 1.3 µm (Kruskal–Wallis H = 8.38 p = 0.015). Maximum and minimum morphometric data of the loricae from each of the geographic areas are summarized in Table S1.

In addition, peculiar micro-alterations have been identified on the surface of the skeleton of the Caribbean scleractinian genera at locations where *Halofolliculina* ciliates were present (Fig. 5a). The ciliates appear to modify the growth pattern of the host coral, apparently eroding part of the skeleton and producing a round-shaped trace where the ciliates were located (Fig. 5b, c). This results in distinct footprints or marks on the coral surface attributable to the protozoans settlement. The shape of the footprint appears cylindrical, although generally not

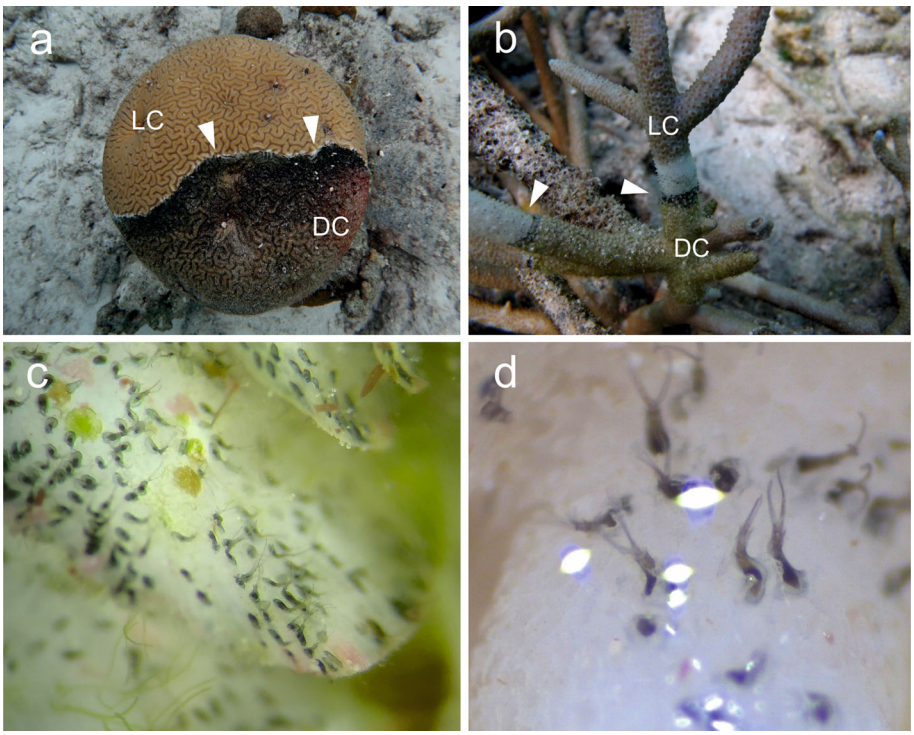

Fig. 2 *Halofolliculina* Ciliate Infection. **a** CCI affecting *Diploria labyrithiformis*; **b** SEB affecting a coral of *Acropora muricata*; **c** close-up of halofolliculinids on a septum of *Eusmilia fastigiata*; **d** close-up of halofolliculinids on a colony of *Acropora muricata*. *LC* live coral; *DC* dead coral; the arrowheads indicate the cluster-like band of protozoans

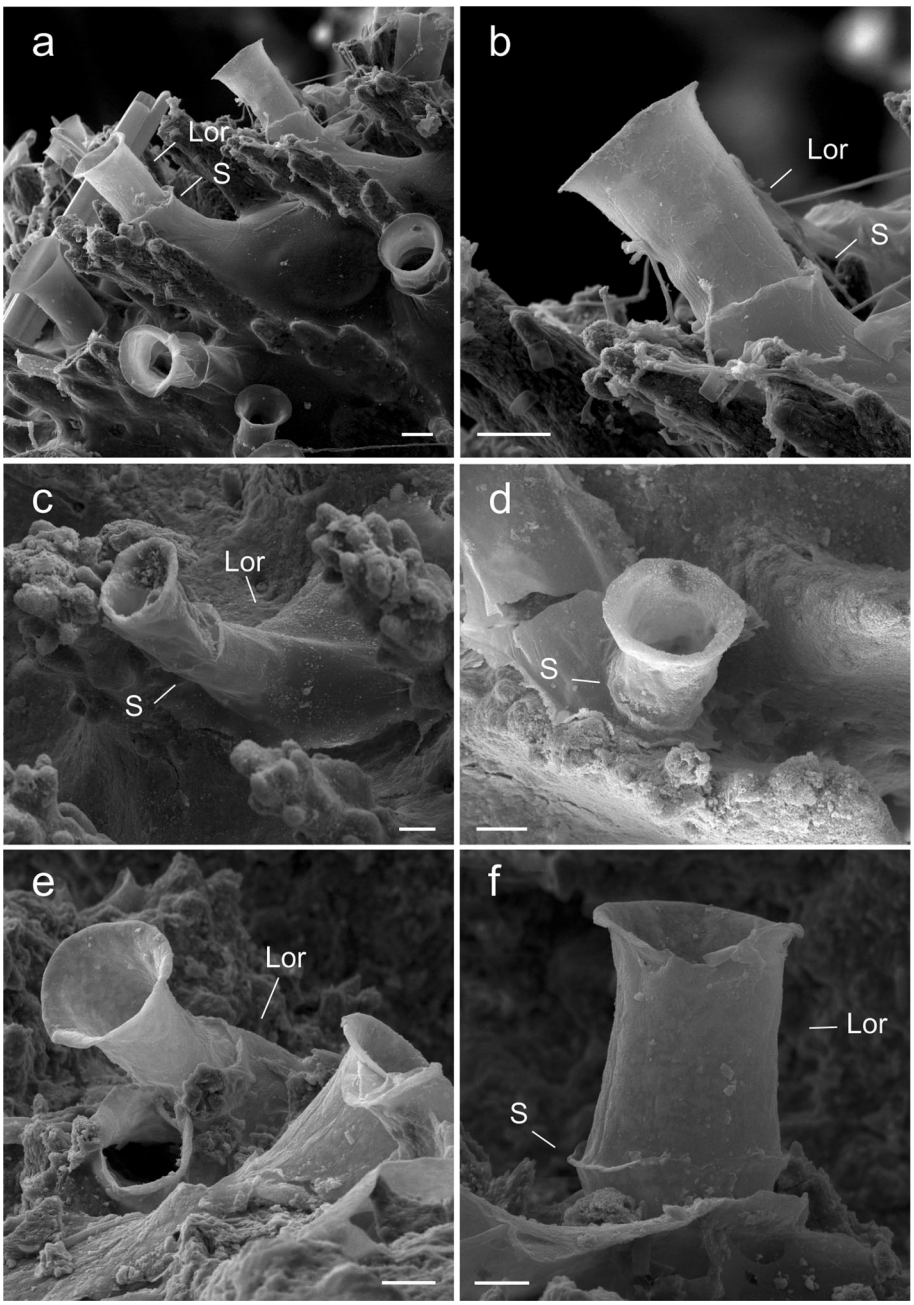

Fig. 3 Various features of *Halofolliculina corallasia* and the peculiar single sculpture (S) of the lorica (Lor) in the three investigated areas: **a**, **b** Indo-Pacific, **c**, **d** Red Sea, **e**, **f** Caribbean. Scale bars: 20 µm

regular, with a diameter ranging from about 50 µm in width to 95 µm in length (Fig. 5d). In some coral colonies, a less evident eroded pattern, ascribable to the presence of the loricae on the skeleton, was also observed (Fig. 5e, f).

Molecular results

The total alignments of the ITS and COI datasets after the Gblocks treatment were 455 and 688 bp long, and consisted in 36 and 40 sequences, respectively. BI and ML analyses resulted in almost identical phylogenetic trees, and therefore only the ML topologies are shown in Fig. 4, with nodal supports indicated as Bayesian posterior probabilities (BPP) and bootstrap supports (BS). The ITS tree (Fig. 6a) shows an overall moderate to good nodal support for the Bayesian analysis, whereas the ML analysis resulted in less supported relationships. All included genera are monophyletic, but a few species are not. The *Halofolliculina* sequences obtained from different localities form a monophyletic clade (BPP = 0.88, BS = 89), sister to *Folliculina simplex* (BPP = 0.99, BS = 84), the only other folliculinid included in the analysis. The evolutionary

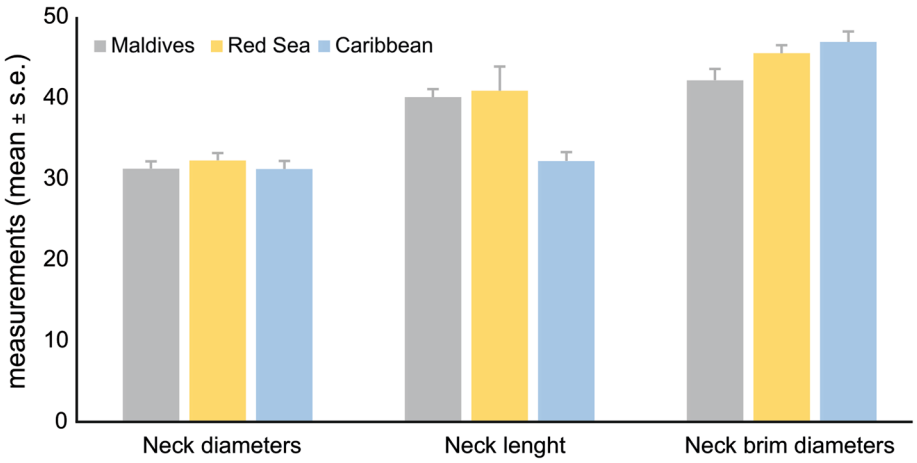

Fig. 4 Mean values and SE of the neck diameter, neck length and the neck brim diameters of the *Halofolliculina* loricae affecting Indo-Pacific (Maldive and Red Sea) and Caribbean scleractinians. Mean values are expressed in μm

relationships represented in the COI tree (Fig. 6b) show higher support values for both BI and ML analyses at genus and species level, but deeper nodes are generally less supported. However, all genera and species included in the analysis are monophyletic, including the *Halofolliculina* clade (BPP = 1, BS = 100). In comparison with the ITS analyses, the halofolliculinids collected from different localities show a higher diversification, and three geography-related, fully supported lineages can be identified.

Genetic distances calculated between heterotrich species and genera are generally high, especially for the COI dataset (Table S2). The average distances between genera and species for the COI dataset are 39.9% (28.5–58.5%) and 32% (8.6–59.1%), respectively, with *Halofolliculina* showing the highest distances towards all other sequences (Table S2). Distances between genera and species in the ITS dataset are lower, being 21.8% (13.1–38.7%) and 18% (0.4–39.4%), respectively (Table S2). The intra-specific distances are higher for the COI dataset, ranging from 0 to 14%, whereas they are lower for the ITS dataset (0.1–7.3%) (Table S2). Regarding the *Halofolliculina* sequences, intra-genus distances are moderately high for the COI (14 ± 0.9%), but very low for the ITS (0.5 ± 0.4). The genetic distances between *Halofolliculina* samples from the three localities are high, ranging from 18.6 to 21.1% (Table S2).

Discussion

The present work reveals the relationship between *Halofolliculina* ciliate infections known as skeletal eroding band in the Indo-Pacific and as Caribbean ciliate infection in the Caribbean, by the application for the first time, of an integrative, morphological molecular approach. Coral lesions and protozoans in the three geographic areas showed the same macroscopic appearance.

In all investigated affected coral species, halofolliculinid infestations manifested themselves as areas of tissue loss and bare skeleton covered by loricae. *Halofolliculina* ciliates settle in clusters following the rim of the corallites and represent dark dots, giving the skeleton a scattered appearance. When in high densities, they form a thick band (1–10 cm), usually black or dark green in colour, between recently exposed skeleton and dead tissue. They can also form more speckled bands when in low density and be more light green in colour. Thus, the in vivo observation of halofolliculinids confirmed the previous information reported for the skeletal eroding band disease (Antonius and Lipscomb 2001; Winkler et al. 2004; Page and Willis 2008) and the Caribbean ciliate infection (Cróquer et al. 2006a). In particular, the analysis of the main features of the protozoans' body and lorica matched with the description of *Halofolliculina corallasia* provided by Antonius and Lipscomb (2001) for all specimens analysed. Moreover, a detailed analysis of the skeleton revealed an erosion on Caribbean diseased corals, suggesting for the first time settlement patterns similar to those of Indo-Pacific SEB-affected corals. In particular, slightly eroded marks related to the presence of *Halofolliculina* loricae have been observed on the Caribbean skeletons, revealing that the ciliate may use the same mechanisms as in Indo-Pacific SEB-causing ciliates. Indeed, the Caribbean *Halofolliculina* ciliates seems to manifest an apparently chemical activity by leaving "sack-shaped" borings or an "honeycomb" pattern while attach their bodies on the coral skeleton as already reported for the Indo-Pacific counterpart (Riegl and Antonius 2003). The footprints were consistent with the position and size of the loricae of *H. corallasia*, although apparently different erosion degree

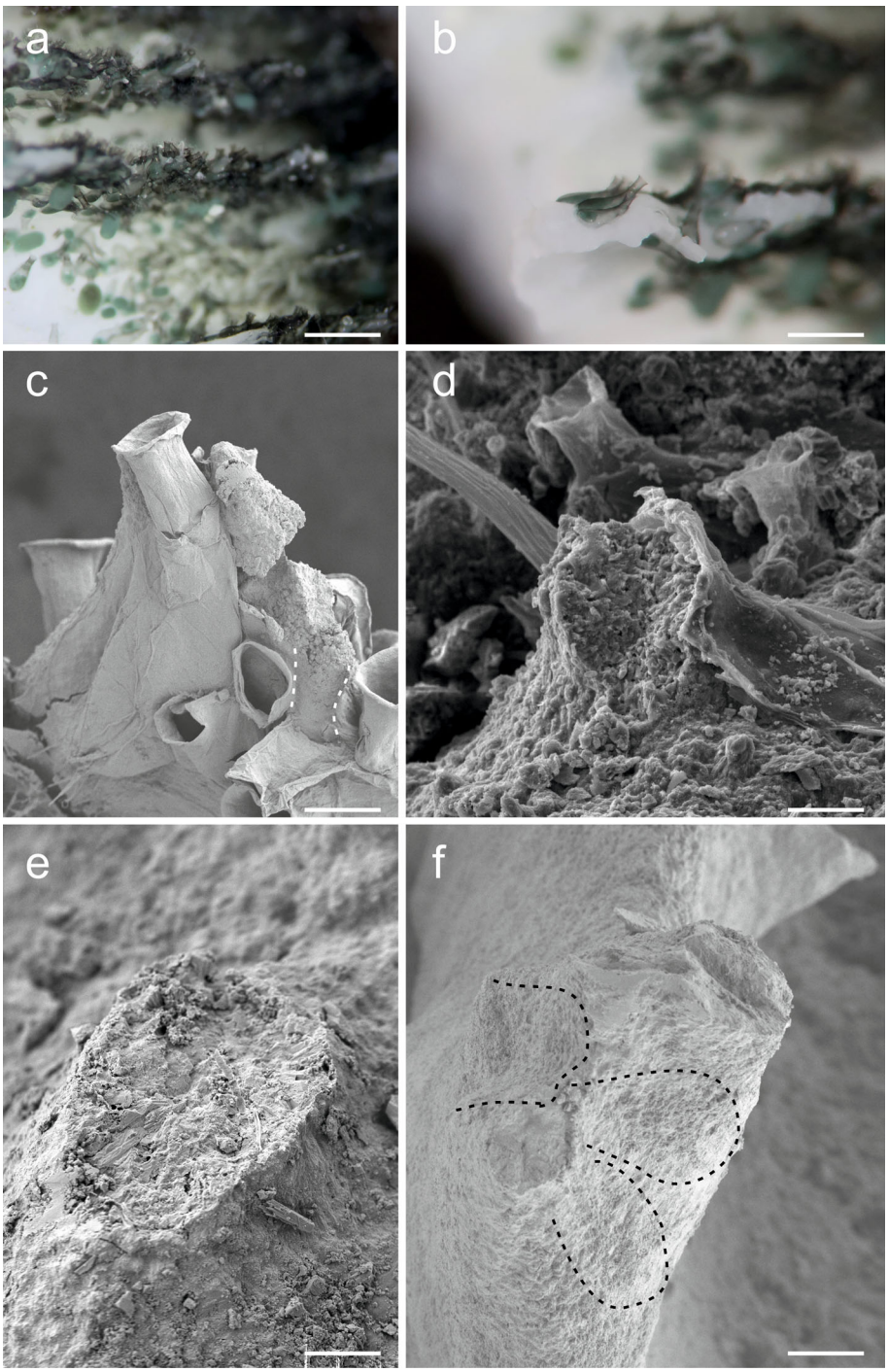

Fig. 5 Scanning electron microscopy images of Caribbean skeletal eroding pattern. **a** Cluster of *Halofolliculina* ciliates on septae of *Diploria labyrinthiformis*; **b** Close-up of loricae apparently eroding the host skeleton; **c** The white dashed line show the eroding pattern left by *Halofolliculina* ciliates on a colony of *Diploria labyrinthiformis*; **d** The round-shaped footprint of the loricae settlement observed on the same host; **e** Apparently different eroding patterns associated to halofolliculinids; **f** Black dashed line show slight footprints related to the presence of halofolliculinids. Scale bars: **a** 1 mm, **b** 0.5 mm, **c**, **d** 50 μm, **e** 10 μm, **f** 20 μm)

within the same samples or host has been detected. If this is related to the time they remain attached to the coral hosts or if some other unknown factors are involved needs to be elucidated in future research.

The main character used to distinguish *H. corallasia* from its congeners is the presence of a single sculpture line circumscribing the neck of the lorica (Antonius and Lipscomb 2001; Page et al. 2015). The single line was evident and easily detectable in all examined protozoans from the Indo-Pacific, Red Sea and the Caribbean. In addition, all the obtained measures fall within the ranges estimated for *H. corallasia* in its first description (Antonius and Lipscomb 2001). Statistical analyses revealed no significant differences in the neck diameter and length, supporting the fine-scale morphological similarities of halofolliculinids from the Caribbean and Indo-Pacific. Although a statistical

difference was found in the neck brim diameters, we believe this morphological character needs further investigation since, in a few cases, loricae were distorted mainly due to the conservation of the sample and to the great variability in the extensibility of the lorica (Primc-Habdija and Matoničkin 2005), and this may have introduced a bias in the measurements. Therefore, all individuals have morphologically been identified as *H. corallasia*, and protozoans found in the Caribbean appeared to be identical to those causing the SEB in the Indo-Pacific and Red Sea.

Overall, the understanding of the genetic relationships among ciliates is complicated by the incomplete knowledge of their diversity (Strüder-Kypke and Lynn 2010). Indeed, ciliated protozoans are largely underrepresented in current biodiversity estimates for many reasons, such as their small size and the difficulty in their isolation and culture (Kher et al. 2011). In line with this gap of knowledge, no genetic information on *H. corallasia* and the whole genus *Halofolliculina* has been presented so far in the literature, and no sequences have been deposited in public databases. Consequently, the DNA sequences herein obtained are the first molecular data for the entire *Halofolliculina* genus and represent a starting point for future genetic evaluations of the species and related taxa.

The molecular results partially diverge from the morphological characterization, finding relevant differences between protozoans from different localities. Although both nuclear and mitochondrial molecular markers revealed the monophyly of all *H. corallasia* individuals sequenced in this work, ITS and COI markers showed variable levels of variation in protozoans from different localities. The *H. corallasia* intra-specific genetic distance based on the ITS dataset was extremely low, whereas that based on COI was higher. Moreover, genetic distances between *Halofolliculina* from the three different localities were remarkably high. These results agree with previous works on ciliate genetic diversity, in which COI showed a much higher diversification than the ITS region (Gentekaki and Lynn 2009; Fernandes et al. 2016).

According to these molecular results, we may hypothesize two main opposite scenarios. Firstly, we may be dealing with a single species with a circumtropical distribution. Indeed, the high intra-*Halofolliculina* genetic distances observed for the COI fall within the range of intraspecific distances found for other heterotrich species. The interspecific divergence is generally much higher in ciliates than in animals and the genetic distance thresholds used for species delimitation differ greatly among ciliate taxa, being for instance around 1% for *Tetrahymena* spp. and 18% for *Carchesium* spp., based on the COI (Gentekaki and Lynn 2009; Kher et al. 2011). These data suggest that evolution rates can be extremely high in ciliates, and that their intraspecific genetic diversity can vary largely among taxa and could be taxon-specific (Gentekaki and Lynn 2009; Strüder-Kypke and Lynn 2010). Researchers have suggested that a high ciliate genetic diversity can depend on several factors, such as a strong gene flow and the ability of the dispersal phase of these microorganisms to reach large distances (Gentekaki and Lynn 2009). It is also assumed that in population of ciliates highly isolated from each other, a positive correlation exists between their genetic divergence and the geographic distance, such as in the case of *Carchesium polypinum* (Zhang et al. 2006). However, there still is no universal consensus about the possible biogeographic diversification of ciliates. Even if rarely, in some cases ciliates population have been demonstrated to have a genetic structure related to their biogeography (Miao et al. 2004; Katz et al. 2005), and this may also the case of *H. corallasia*.

A second scenario would be the presence of multiple cryptic species with a similar morphology, as already found also in other ciliates (e.g. Strüder-Kypke and Lynn 2010; McManus et al. 2010; Katz et al. 2011; Park et al. 2019). In this latter case, the ITS region would result as inappropriate to distinguish between closely related species, whereas the COI divergence could be explained by the presence of different species living in the three localities. Indeed, the COI genetic distances within *H. corallasia* are comparable or higher than the interspecific divergences within the other genera included in the analyses and show, for instance, patterns similar to those of some *Blepharisma* species, which are well-resolved with COI but not with ITS sequences. Moreover, Maldivian samples are more similar to Caribbean ciliates rather than the Red Sea ones. This seems to contradict the scenario of a circumtropical species with a biogeography-related genetic structure and further support the species complex hypothesis.

Therefore, the morphological and molecular data obtained in this work seem to support more the latter scenario, with the identification of a *H. corallasia* species complex as the pathogen associated with both the Caribbean ciliate infection and skeletal eroding band. Even though it cannot be excluded that the SEB may be sympatric with the CCI in some localities, this would represent an unlikely scenario. The most cautious approach when describing coral diseases would be to proceed with the classification of different syndromes only when clear evidence is presented (Bourne et al. 2015). Since we found an approximately identical morphology at micro- and macroscale in ciliates and lesions from different localities, and since *H. corallasia* may actually be a complex of multiple cryptic species, we believe that in order to reduce further confusion supplementary studies that will clarify if CCI and SEB should be synonymized are strongly required.

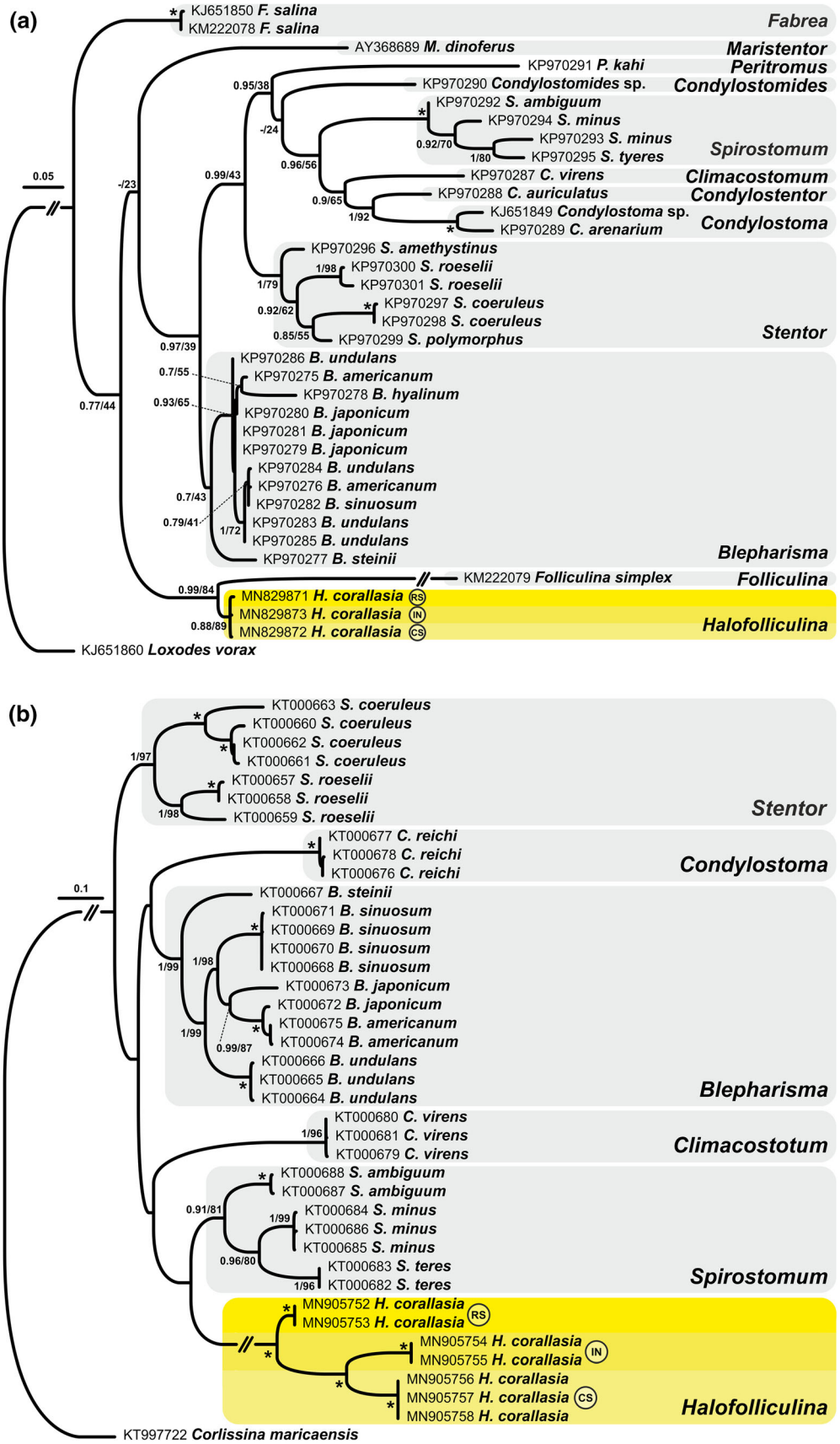
(a)
KJ651850 F. salina
KM222078 F. salina
Fabrea
AY368689 M. dinoferus
Maristentor
KP970291 P. kahi
Peritromus
KP970290 Condylostomides sp.
Condylostomides
KP970292 S. ambiguum
KP970294 S. minus
KP970293 S. minus
KP970295 S. tyeres
Spirostomum
KP970287 C. virens
Climacostomum
KP970288 C. auriculatus
Condylostentor
KJ651849 Condylostoma sp.
KP970289 C. arenarium
Condylostoma
KP970296 S. amethystinus
KP970300 S. roeselii
KP970301 S. roeselii
KP970297 S. coeruleus
KP970298 S. coeruleus
KP970299 S. polymorphus
Stentor
KP970286 B. undulans
KP970275 B. americanum
KP970278 B. hyalinum
KP970280 B. japonicum
KP970281 B. japonicum
KP970279 B. japonicum
KP970284 B. undulans
KP970276 B. americanum
KP970282 B. sinuosum
KP970283 B. undulans
KP970285 B. undulans
KP970277 B. steinii
Blepharisma
KM222079 Folliculina simplex
Folliculina
MN829871 H. corallasia RS
MN829873 H. corallasia IN
MN829872 H. corallasia CS
Halofolliculina
KJ651860 Loxodes vorax
0.05
-/23
0.99/43
0.95/38
-/24
0.96/56
0.92/70
1/80
0.9/65
1/92
1/98
1/79
0.92/62
0.85/55
0.97/39
0.7/55
0.93/65
0.77/44
0.7/43
0.79/41
1/72
0.99/84
0.88/89
(b)
KT000663 S. coeruleus
KT000660 S. coeruleus
KT000662 S. coeruleus
KT000661 S. coeruleus
KT000657 S. roeselii
KT000658 S. roeselii
KT000659 S. roeselii
1/97
1/98
Stentor
KT000677 C. reichi
KT000678 C. reichi
KT000676 C. reichi
Condylostoma
KT000667 B. steinii
KT000671 B. sinuosum
KT000669 B. sinuosum
KT000670 B. sinuosum
KT000668 B. sinuosum
KT000673 B. japonicum
KT000672 B. japonicum
KT000675 B. americanum
KT000674 B. americanum
KT000666 B. undulans
KT000665 B. undulans
KT000664 B. undulans
1/99
1/98
1/99
0.99/87
Blepharisma
KT000680 C. virens
KT000681 C. virens
KT000679 C. virens
1/96
Climacostotum
KT000688 S. ambiguum
KT000687 S. ambiguum
KT000684 S. minus
KT000686 S. minus
KT000685 S. minus
KT000683 S. teres
KT000682 S. teres
0.91/81
1/99
0.96/80
1/96
Spirostomum
MN905752 H. corallasia
MN905753 H. corallasia RS
MN905754 H. corallasia
MN905755 H. corallasia IN
MN905756 H. corallasia
MN905757 H. corallasia CS
MN905758 H. corallasia
Halofolliculina
KT997722 Corlissina maricaensis
0.1

◀**Fig. 6** Phylogenetic trees of *Halofolliculina* and relatives based on the ITS (**a**) and COI (**b**). Numbers at nodes show the Bayesian posterior probabilities and the ML bootstrapping values, respectively. 'Asterisk' indicates that a node is fully supported by both analyses. Halofolliculinids from different localities are highlighted with different shades of yellow; other genera are highlighted in grey. *RS* Red Sea, *IN* Indo-Pacific, *CS* Caribbean Sea

Acknowledgements SM is grateful to Naturalis Biodiversity Center for providing Martin Fellowships, which supported fieldwork in Curaçao (2017) and Bonaire (2019). The fieldwork in Bonaire was also supported by a grant from the WWF-Netherlands Biodiversity Fund to BWH. The staff of CARMABI Marine Research Center at Curaçao is thanked for logistical support. We are grateful to STINAPA and DCNA at Bonaire for assistance in the submission of the research proposal and the research permit.

References

Aeby GS, Ushijima B, Campbell JE, Jones S, Williams GJ, Meyer JL, Häse C, Paul VJ (2019) Pathogenesis of a tissue loss disease affecting multiple species of corals along the Florida Reef Tract. Front Mar Sci 6:678

Antonius A (1999) *Halofolliculina corallasia*, a new coral-killing ciliate on Indo-Pacific reefs. Coral Reefs 18:300

Antonius AA, Lipscomb D (2001) First protozoan coral-killer identified in the Indo-Pacific. Atoll Res Bull 481:1–21

Beli E, Aglieri G, Strano F, Maggioni D, Telford MJ, Piraino S, Cameron CB (2018) The zoogeography of extant rhabdopleurid hemichordates (Pterobranchia: graptolithina), with a new species from the Mediterranean Sea. Invertebr Syst 32:100–110

Bourne DG, Garren M, Work TM, Rosenberg E, Smith GW, Harvell CD (2009) Microbial disease and the coral holobiont. Trends Microbiol 17:554–562

Bourne DG, Ainsworth TD, Pollock FJ, Willis BL (2015) Towards a better understanding of white syndromes and their causes on Indo-Pacific coral reefs. Coral Reefs 34:233–242

Bruno JF, Selig ER (2007) Regional decline of coral cover in the Indo-Pacific: timing, extent, and subregional comparisons. PLoS ONE 2:e711

Casamatta DA, Stani D, Gantar M, Richardson LL (2012) Characterization of *Roseofilum reptotaenium* (Cyano bacteria, Oscillatoriales) gen. et sp. nov. isolated from Caribbean black band disease. Phycologia 51:489–499

Castresana J (2000) Selection of conserved blocks from multiple alignments for their use in phylogenetic analysis. Mol Biol Evol 17:540–552

Cróquer A, Bastidas C, Lipscomp D, Rodríguez-Martínez RE, Jordan-Dahlgren E, Guzman HM (2006a) First report of folliculinid ciliates affecting Caribbean scleractinian corals. Coral Reefs 25:187–191

Cróquer A, Bastidas C, Lipscomb D (2006b) Folliculinid ciliates: a new threat to Caribbean corals?. Dis Aquat Org 69:75–78

Darriba D, Taboada GL, Doallo R, Posada D (2012) jModelTest 2: more models, new heuristics and parallel computing. Nature Methods 9:772

Fernandes NM, da Silva Paiva T, da Silva-Neto ID, Schlegel M, Schrago CG (2016) Expanded phylogenetic analyses of the class Heterotrichea (Ciliophora, Postciliodesmatophora) using five molecular markers and morphological data. Mol Phylogenet Evol 95:229–246

Gardener T, Cote IM, Gill JA, Grant A, Watkinson AR (2003) Long-term region-wide declines in Caribbean corals. Science 301:958–960

Gentekaki E, Lynn DH (2009) High-level genetic diversity but no population structure inferred from nuclear and mitochondrial markers of the peritrichous ciliate Carchesium polypinum in the Grand River basin (North America). Appl Environ Microbiol 75:3187–3195

Hoeksema BW, Koh EGL (2009) Depauperation of the mushroom coral fauna (Fungiidae) of Singapore (1860s–2006) in changing reef conditions. Raffles Bull Zool Suppl 22:91–101

Katoh K, Standley DM (2013) MAFFT multiple sequence alignment software version 7: improvements in performance and usability. Mol Biol Evol 30:772–780

Katz LA, McManus GB, Snoeyenbos-West LO, Griffin A, Pirog K, Costas B, Foissner W (2005) Reframing the "everything is everywhere" debate: evidence for high gene flow and diversity in ciliate morphospecies. Aquat Microb Ecol 41:55–65

Katz LA, DeBerardinis J, Hall MS, Kovner AM, Dunthorn M, Muse SV (2011) Heterogeneous rates of molecular evolution among cryptic species of the ciliate morphospecies Chilodonella uncinata. J Mol Evol 73:266–272

Kher CP, Doerder FP, Cooper J, Ikonomi P, Achilles-Day U, Küpper FC, Lynn DH (2011) Barcoding Tetrahymena: discriminating species and identifying unknowns using the cytochrome c oxidase subunit I (cox-1) barcode. Protist 162:2–13

Kumar S, Stecher G, Li M, Knyaz C, Tamura K (2018) MEGA X: molecular evolutionary genetics analysis across computing platforms. Mol Biol Evol 35:1547–1549

McManus GB, Xu D, Costas BA, Katz LA (2010) Genetic identities of Cryptic species in the Strombidium stylifer/apolatum/oculatum cluster, including a description of Strombidium rassoulzadegani n. sp. J Eukaryotic Microbiol 57:369–378

Meyer JL, Castellanos-Gell J, Aeby GS, Häse C, Ushijima B, Paul VJ (2019) Microbial community shifts associated with the ongoing stony coral tissue loss disease outbreak on the Florida Reef Tract. bioRxiv 626408

Miao W, Yu Y, Shen YH, Zhang X (2004) Intraspecific phylogeography of Carchesium polypinum (Peritrichia, Ciliophora) from China, inferred from 18SITS1-5.8S ribosomal DNA. Sci China 47:11–17

Montano S, Arrigoni R, Pica D, Maggioni D, Puce S (2015) New insights into the symbiosis between *Zanclea* (Cnidaria, Hydrozoa) and scleractinians. Zool Scripta 44:92–105

Page CA, Willis BL (2008) Epidemiology of skeletal eroding band on the Great Barrier Reef and the role of injury in the initiation of this widespread coral disease. Coral Reefs 27:257–272

Page CA, Cróquer A, Bastidas C, Rodríguez S, Neale SJ, Weil E, Willis BL (2015) *Halofolliculina* ciliate infections on corals (skeletal eroding disease). In: Woodley CM, Downs CA, Bruckner AW, Porter JW, Galloway SB (eds) Diseases of Coral. Wiley-Blackwell, Hoboken, pp 361–375

Park MH, Jung JH, Jo E, Park KM, Baek YS, Kim SJ, Min GS (2019) Utility of mitochondrial CO1 sequences for species discrimination of Spirotrichea ciliates (Protozoa, Ciliophora). Mitochondrial DNA Part A 30:148–155

Pollock FJ, Morris PJ, Willis BL, Bourne DG (2011) The urgent need for robust coral disease diagnostics. PLoS Pathogens 7(10):e1002183

Primc-Habdija B, Matoničkin R (2005) A new freshwater folliculinid (Ciliophora) from the karstic region of Croatia. Eur J Protistol 41:37–43

Rambaut A (2012) Figtree v 1.4.0. http://tree.bio.ed.ac.uk/software/figtree/. Accessed 21 June 2019

Riegl B, Antonius A (2003) *Halofolliculina* skeleton eroding band (SEB): a coral disease with fossilization potential? Coral Reefs 22:48

Rodríguez S, Croquer A, Guzmán HM, Bastidas C (2009) A mechanism of transmission and factors affecting coral susceptibility to *Halofolliculina* sp. infection. Coral Reefs 28:67–77

Ronquist F, Teslenko M, van der Mark P, Ayres DL, Darling A, Höhna S, Larget B, Liu L, Suchard MA, Huelsenbeck JP (2012) MrBayes 3.2: efficient Bayesian phylogenetic inference and model choice across a large model space. Syst Biol 61:539–542

Rosenberg E, Kelloff CA, Rohwer F (2007) Coral microbiology. Oceanography 20:146–154

Sutherland WJ, Clout M, Depledge M, Dicks LV, Dinsdale J, Entwistle AC, Fleishman E, Gibbons DW, Keim B, Lickorish FA, Monk KA, Ockendon N, Peck LS, Pretty J, Rockström J, Spalding MD, Tonneijck FH, Wintle BC (2015) A horizon scan of global conservation issues for 2015. Trends Ecol Evol 30:17–24

Sussman M, Bourne DG, Willis BL (2006) A single cyanobacterial ribotype is associated with both red and black bands on diseased corals from Palau. Dis Aquat Organ 69:111–118

Stamatakis A (2006) RAxML-VI-HPC: maximum likelihood-based phylogenetic analyses with thousands of taxa and mixed models. Bioinformatics 22:2688–2690

Stamatakis A (2014) RAxML version 8: a tool for phylogenetic analysis and post-analysis of large phylogenies. Bioinformatics 30:1312–1313

Strüder-Kypke MC, Lynn DH (2010) Comparative analysis of the mitochondrial cytochrome c oxidase subunit I (COI) gene in ciliates (Alveolata, Ciliophora) and evaluation of its suitability as a biodiversity marker. Syst Biodivers 8:131–148

Sun P, Clamp JC, Xu D (2010) Analysis of the secondary structure of ITS transcripts in peritrich ciliates (Ciliophora, Oligohymenophorea): implications for structural evolution and phylogenetic reconstruction. Mol Phylogenet Evol 56:242–251

Sweet JM, Séré GM (2015) Ciliate communities consistently associated with coral diseases. J Sea Res 113:119

Talavera G, Castresana J (2007) Improvement of phylogenies after removing divergent and ambiguously aligned blocks from protein sequence alignments. Syst Biol 56:564–577

Weil E, Hooten, AJ (2008) Underwater cards for assessing coral health on Caribbean reefs. Coral reefs targeted research and capacity building for management, 24-pp

Weil E, Rogers CS (2011) Coral reef diseases in the Atlantic-Caribbean. In: Dubinsky Z, Stambler N (eds.) Coral Reefs: An Ecosystem in Transition. Springer, Dordrecht, Netherlands, pp 465–491

Willis BL, Page CA, Dindsdale EA (2004) Coral disease in the great barrier reef. In: Rosenberg E, Loya Y (eds) Coral health and disease. Springer, Berlin, pp 69–104

Winkler R, Antonius A, Abigail Renegar D (2004) The skeleton eroding band disease on coral reefs of Aqaba, Red Sea. Mar Ecol 25:129–144

Work T, Meteyer C (2014) To understand coral disease, look at coral cells. EcoHealth 11:610–618

Yi Z, Song W (2011) Evolution of the order Urostylida (Protozoa, Ciliophora): new hypotheses based on multi-gene information and identification of localized incongruence. PLoS ONE 6:e17471

Zar JH (1999) Biostatistical analysis. Prentice-Hall, London

Zhang WJ, Yang J, Yu YH, Shu SW, Shen YF (2006) Population genetic structure of Carchesium polypinum (Ciliophora: Peritrichia) in four Chinese lakes inferred from ISSR fingerprinting: high diversity but low differentiation. J Eukaryot Microbiol 53:358–363